Chinese Chemical Letters 32 (2021) 516–520

Contents lists available at ScienceDirect

Chinese Chemical Letters

journal homepage: www.elsevier.com/locate/cclet

Communication

Cooperation between Pt and Ru on RuPt/AC bimetallic catalyst in the hydrogenation of phthalates

Yan Xu[a], Chenguang Wu[a], Yan Wang[a], Ying Zhang[a], Han Sun[b], Haijun Chen[b], Yujun Zhao[a,*]

[a] Key Laboratory for Green Chemical Technology of Ministry of Education, Collaborative Innovation Center of Chemical Science and Engineering, School of Chemical Engineering and Technology, Tianjin University, Tianjin 300072, China
[b] College of Electronic Information and Optical Engineering, Nankai University, Tianjin 300350, China

ARTICLE INFO

Article history:
Received 1 March 2020
Received in revised form 14 March 2020
Accepted 8 April 2020
Available online 18 April 2020

Keywords:
Ru
RuPt alloy
Bimetallic catalyst
Phthalates
Hydrogenation

ABSTRACT

RuPt/AC bimetallic catalysts were prepared by two-step incipient impregnation method and evaluated in the hydrogenation of phthalates. According to the characterization results, well dispersed RuPt bimetallic nanoparticles were formed on the catalyst, and the strong interaction between the two metals resulted in the formation of RuPt alloy. It was found that Ru can donate electrons to Pt on RuPt alloy nanoparticles, leading to the formation of electron-deficient Ru which significantly promotes the hydrogenation rate of dioctyl phthalate and improves the selectivity of dioctyl di-2-ethylhexylcyclohexane-1,4-dicarboxylate by accelerating the further hydrogenation of intermediate products. The bimetallic RuPt catalyst also presented excellent stability and versatility in the hydrogenation of phthalates, demonstrating its prospective future in the hydrogenation of aromatic ring contained compounds.

In recent years, the effect of phthalates has become one of the major public health concerns [1–3]. Cyclohexane dicarboxylic acid ester is benzol-free ester, which can be produced by phthalates hydrogenation. Some research showed that cyclohexane dicarboxylic acid ester has better performance on plasticity and safety, and it is becoming an environment-friendly plasticizer to replace phthalates [4,5].

Bimetallic catalyst is always used in some reaction system as a result of its higher activity and selectivity. Qu *et al.* [6] designed bimetallic RuRe catalyst for selective hydrogenation of dimethyl terephthalate (DMT) to 1,4-cyclohexane dicarboxylate (DMCD). The distribution of active metal species on the surface was greatly improved by the addition of Re, at the same time Re promoted the charge transfer between Ru and Re and strengthened the RuRe synergistic interaction. Zhang *et al.* [7–9] reported that bimetallic RuPd prevented the nanoparticle aggregation and the structure of NiAlRu-layered double hydroxide endowed the higher metal dispersion and Ru facilitate the reduction of Ni^{2+} because of the hydrogen spillover.

Li *et al.* [10] found that $RuSn/Al_2O_3$ catalyst was not a suitable catalyst to produce 1,4-cyclohexanedimethanol (CHDM) *via* one-pot hydrogenation of DMT, because the introduction of Sn metal restrained the hydrogenation capability of Ru catalyst. However, when Pt metal is introduced into the $RuSn/Al_2O_3$ catalyst, the ability of Ru in the hydrogenation of phenyl group is enhanced obviously, resulting a higher yield to the designed alcohol CHDM. They suggested that the introduction of Pt into the bimetallic RuSn catalyst may enhance the reducibility and dispersion of the metal particles.

In previous work [11], we found that monometallic Ru/AC catalyst with appropriate microporous structure exhibited excellent activity in the hydrogenation of various phthalates. However, under mild reaction conditions the Ru/AC catalyst has lower selectivity of dioctyl di-2-ethylhexylcyclohexane-1,4-dicarboxylate (DEHCH) due to its lower activity in the further hydrogenation of the bis(2-ethylhexyl) cyclohexene-1,2-dicarboxylate (4H-DOP), which is an intermediate product of dioctyl phthalate (DOP) hydrogenation. Therefore, how to improve the hydrogenation activity of Ru is the key for developing highly efficient catalyst. The addition of second metal such as Pt could help improving the hydrogenation ability of Ru in DOP hydrogenation to DEHCH. An insight into the possible synergistic effect between Pt and Ru could give some rational direction for this reaction system.

Herein, a series of bimetallic RuPt/AC catalysts were prepared by two-step incipient impregnation with the activated carbon as

* Corresponding author.
E-mail address: yujunzhao@tju.edu.cn (Y. Zhao).

https://doi.org/10.1016/j.cclet.2020.04.016

the support and applied for DOP hydrogenation (details can be found in Supporting information). It was found that bimetallic RuPt catalyst showed much higher activity and selectivity than monometallic Ru or Pt catalysts due to the electron transfer between Ru and Pt.

Pore structure distribution curves and N_2 adsorption-desorption isotherm are shown in Figs. S1A–C (Supporting information). All the samples show type IV adsorption isotherm and type H4 hysteresis loop, in accordance with the categorization of IUPAC, which are typical characteristics of micro-mesoporous materials [12,13]. As listed in Table S1 (Supporting information), all catalysts present the identical pore volume, specific surface area and the average pore size as a result of the lower metal loading (both Pt and Ru) [14]. The similar structure of various catalysts excludes the difference in mass transfer.

Fig. S1D (Supporting information) shows the X-ray diffraction (XRD) patterns of the $RuPt_x$/AC with various Pt/Ru mole ratio (x = 0, 0.3, 0.6, 1.2). No significant difference in the diffraction peaks of these samples. All the XRD patterns of these samples show two broad peaks near 23° and 44°, belonging to (002) and (100) planes of typical amorphous carbon [15]. It indicates that the structure of the initial activated carbon is basically maintained during the preparation of the catalysts. The characteristic diffraction peaks of Ru [16,17] and Pt [18] particles are not observed, implying that both Ru and Pt are highly dispersed on AC carriers [19,20].

CO pulse chemisorption was used to characterize the Ru dispersion and particle sizes for all the catalysts. As listed in Table 1, with the increase of Pt content, the metal dispersion gives a slight decrease. During the two-step incipient impregnation process for the catalyst preparation, Ru particles could deposit around Pt particles, and finally formed RuPt nanoparticles after reduction. Therefore, the increase of Pt content resulted in larger RuPt nanoparticles.

The size of $RuPt_x$ nanoparticle was measured by transmission electron microscope (TEM). It can be seen from Fig. 1 that all these catalysts show the disordered structure of amorphous carbon, corresponding to the above XRD results. The overview images of Ru/AC, $RuPt_{0.3}$/AC, $RuPt_{0.6}$/AC and $RuPt_{1.2}$/AC (Fig. 1) reveal that the catalysts with a Pt/Ru ratio of less than 1.2 can ensure the high dispersion of RuPt nanoparticles on the carbon support, while much higher ratio of Pt/Ru led to the severe aggregation of RuPt nanoparticles (*e.g.*, $RuPt_{1.2}$/AC catalyst). Similarly, the distribution histograms of RuPt nanoparticle size show that the nanoparticle size of RuPt increases with the content of Pt. The average nanoparticle sizes of Ru/AC, $RuPt_{0.3}$/AC, $RuPt_{0.6}$/AC and $RuPt_{1.2}$/AC are 2.51, 3.44, 3.96 and 6.60 nm, respectively, which agrees well with the results of CO pulse chemisorption. Energy dispersive spectroscopy (EDS) mapping images of the $RuPt_{0.6}$/AC catalyst are shown in Fig. 1F and Fig. S2 (Supporting information), both Pt (green) and Ru (red) exhibit almost the similar element distribution, allowing the possible formation of RuPt alloy [21,22].

In order to insight into the chemical nature of the metal phases on the catalysts surface, X-ray photoelectron spectroscopy (XPS) analysis was carried out on the $RuPt_x$/AC catalysts, as well as the Pt/AC and Ru/AC monometallic catalysts. The binding energies are listed in Table 1. As shown in Fig. 2A, the peak intensity of $RuPt_x$/AC is lower than that of Pt/AC, which should be ascribed to the lower content of Pt and the confinement of Pt in the lattice of Ru. Moreover, the binding energies of Pt^0 on $RuPt_x$/AC shift to lower binding energy ($4f_{7/2}$ at 71.37–71.43 eV) in comparison with that ($4f_{7/2}$ at 71.69 eV) on Pt/AC. The negative migration of binding energy of Pt $4f_{7/2}$ in $RuPt_x$/AC is because of the electron contribution of Ru to Pt. Because Ru $3d_{3/2}$ region can overlap with C ls region at around 284.5 eV, the $3d_{5/2}$ region of Ru are investigated for carbon supported Ru catalyst. The Ru $3d_{5/2}$ region in Fig. 2B identify that ruthenium is presented in a state of both Ru° ($3d_{5/2}$ at 280.53 eV) and Ru^{4+} ($3d_{5/2}$ at 281.14 eV, oxidized during sample preparation at room temperature in air [23]) on the catalyst surface. Compared with the Ru/AC (280.52 eV), the binding energies of the Ru^0 in $RuPt_x$/AC shift slightly to higher energies (280.61 eV), suggesting Ru donates electrons to Pt. The interaction between the two metals indicates the possible formation of RuPt alloy on the surface of bimetallic catalyst.

The H_2 temperature programmed reduction (TPR) results of various catalysts are shown in Fig. 3. No obvious reduction peak can be found in the TPR pattern of Pt/AC, implying that most of Pt species on Pt/AC has been reduced by the surface reductive species on AC during the calcination in N_2 environment. However, there are two reduction peaks at 283 °C and 163 °C for Ru/AC catalyst, which should belong to the RuO_x having strong interaction with support and highly dispersed RuO_x, respectively [24–26]. Moreover, in the case of $RuPt_x$/AC catalysts, the second reduction peak of RuO_x is disappeared, demonstrating that the interaction between Ru nanoparticles and support has changed due to the presence of Pt. The close contact between Pt and Ru could promote the reduction of RuO_x since metallic Pt can accelerate the hydrogen activation and spillover to adjacent RuO_x. Thus, the formation of RuPt alloy nanoparticles can be enhanced during this reduction process [27]. This result agrees well with the XPS and HRTEM results.

In order to clarify the catalysis nature of RuPt alloy nanoparticles in the DOP hydrogenation on various catalysts, a series of experiments were carried out in a stirred tank reactor. As listed in Table 2, Pt/AC shows much lower conversion (2.5%) than Ru/AC catalyst (39.9%), indicating the less activity of Pt than Ru in DOP hydrogenation. However, the introduction of Pt significantly improved the DOP conversion of Ru catalyst, and a much higher conversion of about 56.7% is achieved on $RuPt_{0.6}$/AC bimetallic catalyst. Therefore, we believe that Ru instead of Pt is the active

Table 1
Dispersion, particle diameter and Ru Pt binding energy of the catalysts.

Catalysts	Metal dispersion[a] (%)	D_A[a] (nm)	D_A[b] (nm)	Binding energy[c] (eV)		
				Pt $4f_{5/2}$	Pt $4f_{7/2}$	Ru $3d_{5/2}$
Pt/AC	–	–	–	75.01	71.69	–
Ru/AC	30.6	2.94	2.51	–	–	280.52
$RuPt_{0.3}$/AC	27.9	3.43	3.44	74.87	71.43	280.52
$RuPt_{0.6}$/AC	24.2	4.08	3.96	74.83	71.37	280.57
$RuPt_{1.2}$/AC	19.2	5.35	6.60	74.79	71.37	280.61

[a] Determined by CO pulse chemisorption.
[b] Determined by transmission electron microscope (TEM).
[c] Determined by X-ray photoelectron spectroscopy (XPS).

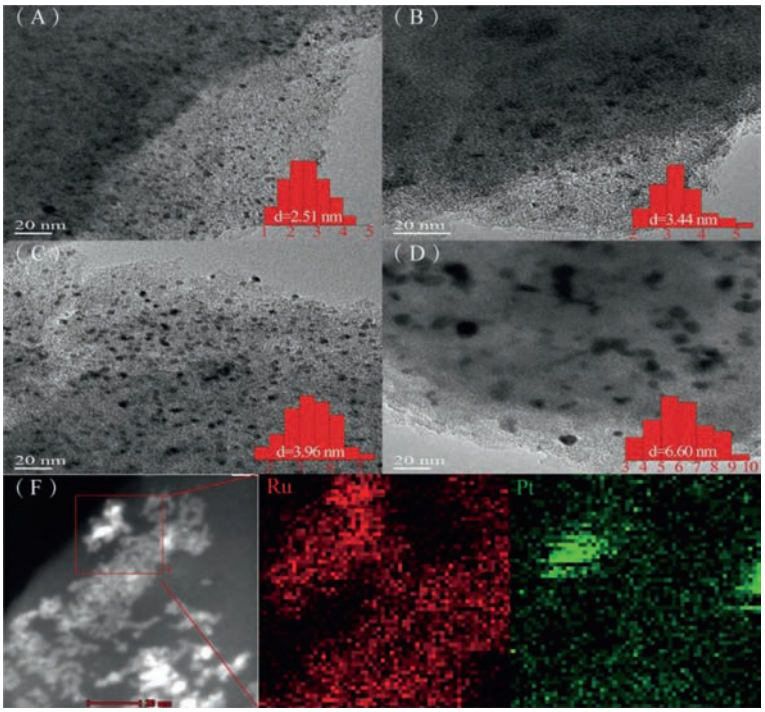

Fig. 1. High resolution TEM (HRTEM) images of Ru/AC (A), $RuPt_{0.3}$/AC (B), $RuPt_{0.6}$/AC (C), $RuPt_{1.2}$/AC (D) catalysts and EDS mapping image of the $RuPt_{0.6}$/AC catalyst (F).

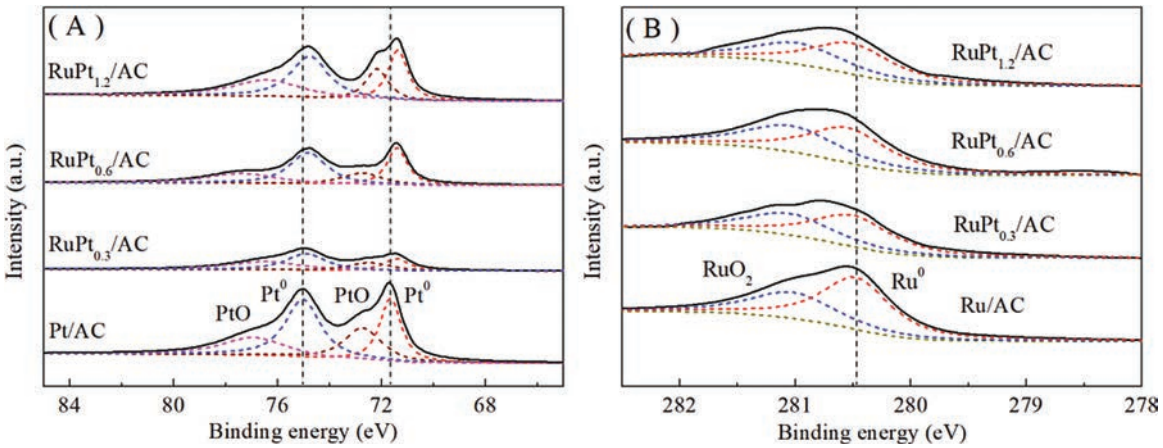

Fig. 2. XPS spectra of Pt 4f (A) and Ru 3d (B) for $RuPt_x$/AC catalysts.

specie of the catalyst at the given reaction conditions. Meanwhile, as shown in Fig. S3 (Supporting information), an excess amount of Pt will also result in a decrease of activity, probably due to the agglomeration of RuPt nanoparticles. Therefore, the highest activity can be obtained at the optimized Pt/Ru ratio of 0.6. In addition, the selectivity of DEHCH is significantly improved from 63.7% on Ru/AC to 83.2% on $RuPt_{0.6}$/AC, implying the promoting effect of PtRu alloy on the further hydrogenation of the intermediate product 4H-DOP with only single C=C bond. Their TOF value further demonstrates that the formation of PtRu alloy significantly improves the activity of Ru active site on the conversion of DOP (Fig. S4 in Supporting information shows that the reaction rate is constant at the conversion below 60%). On basis of the XPS and TPR results, the electronic transfer from Ru to Pt leads to the formation of electron-deficient Ru, which could promote the hydrogenation rate of 4H-DOP and improves the DEHCH selectivity.

Hydrogenation of various phthalates including DOP, dipentyl phthalate (DPP) and dimethyl phthalate (DMP) were examined on $RuPt_{0.6}$/AC and Ru/AC catalysts. As listed in Table S2 (Supporting information), the two catalysts show different activity in the hydrogenation of various model reactants, and their TOFs exhibit a decrease trend with the increase of the reactant molecular size. In addition, $RuPt_{0.6}$/AC is much more active than Ru/AC in the hydrogenation of all phthalates due to the Ru-Pt interaction.

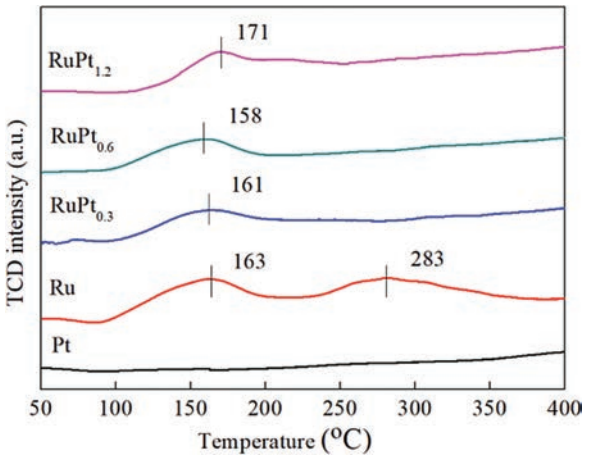

Fig. 3. H_2-TPR profiles of the Ru/AC, Pt/AC and $RuPt_x$/AC catalysts.

Table 2
Hydrogenation of DOP on the $RuPt_x$/AC Catalysts.

Catalysts	Conversion (%)	Selectivity[a] (%)	Selectivity[b] (%)	TOF (h^{-1})
AC[c]	0.0	0.0	0.0	–
Pt + Ru/AC[d]	21.5	57.1	42.9	–
Pt/AC	2.5	44.3	55.7	–
Ru/AC	39.9	62.7	37.3	3015
$RuPt_{0.3}$/AC	50.6	82.6	17.4	4349
$RuPt_{0.6}$/AC	56.7	83.2	16.8	5142
$RuPt_{1.2}$/AC	43.9	47.9	20.4	5194

[a] DEHCH selectivity.
[b] 4H-DOP selectivity.
[c] Only active carbon support.
[d] Mechanical mixture of Pt/AC and Ru/AC.

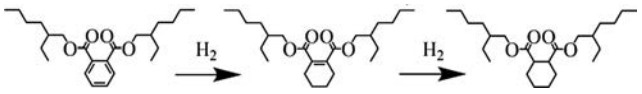

Scheme 1. Reaction route for DOP hydrogenation.

Figs. S5 and S6 (Supporting information) show the products distribution obtained on the Ru/AC and $RuPt_{0.6}$/AC catalysts. For both the two catalysts, the concentration of 4H-DOP is first increased and then decreased to 0% with the time (Fig. S5A in Supporting information), while the total hydrogenation product DEHCH presents an increasing trend until its selectivity reaches 100% (Fig. S6B in Supporting information). It strongly evidences that the liquid-phase hydrogenation of DOP follows a consecutive reaction route as illustrated in Scheme 1. This result agrees well with the findings reported by Duc Ha *et al.* [28] on the hydrogenation of DMP. For the Ru-based catalyst, the further hydrogenation of the intermediate 4H-DOP could be the determining step for this consecutive reaction. The bimetallic RuPt catalyst is more active than the monometallic one due to the superior activity in the hydrogenation of intermediate. On this catalyst, the Ru site decorated by Pt is much more active than single Ru or Pt site in the hydrogenation of aromatic ring, especially in the saturation of 4H-DOP with single C=C bond. Thus, the cooperation between Pt and Ru significantly enhances the reaction rate of 4H-DOP hydrogenation, accompanied by the formation of DEHCH.

The bimetallic RuPt catalyst exhibits a stable activity during the reusage in DOP hydrogenation (Fig. S7 in Supporting information). Moreover, it also presents excellent catalytic performance and versatility in various phthalates' hydrogenation (Table S3 in Supporting information). These results demonstrate the prospective future of the bimetallic RuPt catalyst in the synthesis of environment-friendly plasticizer *via* phthalates hydrogenation.

In summary, the hydrogenation of phthalates to environment-friendly plasticizers is becoming an attractive issue from both the academic and industrial fields. This work prepared a series of $RuPt_x$/AC catalysts for the DOP hydrogenation and the mechanism of RuPt alloy nanoparticle is well discussed and proposed. It was found that both the metals were highly dispersed on the AC support and the interaction between Ru and Pt led to formation of RuPt alloy nanoparticles during the reduction. However, an excess amount of Pt can result in the agglomeration of RuPt nanoparticles. The as-prepared RuPt/AC bimetallic catalyst exhibited a superior catalytic activity than monometallic Ru/AC or Pt/AC catalyst, which is ascribed to the formation of RuPt alloy in the RuPt bimetallic catalyst. It was proposed that Ru can donate electron to Pt in RuPt nanoparticles, resulting in electron-deficient Ru sites which significantly promote the hydrogenation rate of DOP and improve the DEHCH selectivity by enhancing the deep hydrogenation of intermediate products. The RuPt bimetallic catalyst presented excellent stability during the reusage in batch reactor and exhibited promising versatility in phthalates hydrogenation. These findings demonstrate a prospective future of the RuPt/AC bimetallic catalyst in the selective hydrogenation of aromatic ring contained compounds.

Declaration of competing interest

The authors declare that there are no conflicts of interest.

Acknowledgment

We appreciate the National Natural Science Foundation of China (Nos. 21878227, 21276186) for the financial support.

Appendix A. Supplementary data

Supplementary material related to this article can be found, in the online version, at doi:https://doi.org/10.1016/j.cclet.2020.04.016.

References

[1] Z.L. Ye, C.Q. Cao, J.C. He, R.X. Zhang, H.Q. Hou, Chin. Chem. Lett. 20 (2009) 706–710.
[2] J. Li, Y. Li, Z. Xiong, G. Yao, B. Lai, Chin. Chem. Lett. 30 (2019) 2139–2146.
[3] A. Jankowska, K. Polańska, H.M. Koch, et al., Environ. Res. 179 (2019) 108829.
[4] A. Schuetze, C. Paelmke, J. Angerer, et al., J. Chromatogr. B-Analyt. Technol. Biomed. Life Sci. 895 (2012) 123–130.
[5] B.L. Wadey, J. Vinyl Add. Technol. 9 (2003) 172–176.
[6] E. Qu, J. Luo, X. Di, C. Li, C. Liang, J. Nanosci. Nanotechnol. 20 (2020) 1140–1147.
[7] J. Chen, X. Liu, F. Zhang, Chem. Eng. J. 259 (2015) 43–52.
[8] Z. Yang, J. Han, Q. Fan, H. Jia, F. Zhang, Appl. Catal. A: Gen. 568 (2018) 183–190.
[9] H. Jia, Z. Yang, X. Yun, et al., Ind. Eng. Chem. Res. 58 (2019) 22702–22708.
[10] X. Li, Z. Sun, J. Chen, Y. Zhu, F. Zhang, Ind. Eng. Chem. Res. 53 (2014) 619–625.
[11] Y. Xu, Y. Wang, C. Wu, et al., Catal. Commun. 132 (2019) 105825.
[12] Z. Zhao, T. Bao, Y. Zeng, G. Wang, T. Muhammad, Catal. Commun. 32 (2013) 47–51.
[13] N. Gong, Z. Zhao, Mol. Catal. 477 (2019) 110543.
[14] K. Xiong, J. Li, K. Liew, X. Zhan, Appl. Catal. A: Gen. 389 (2010) 173–178.
[15] J. Zhang, J. Wang, Z. Shi, Z. Xu, Chin. Chem. Lett. 29 (2018) 620–623.
[16] J.Y. Park, Y.J. Lee, P.R. Karandikar, et al., J. Mol. Catal. A: Chem. 344 (2011) 153–160.
[17] P.P. Upare, M. Lee, S.K. Lee, et al., Catal. Today 265 (2016) 174–183.
[18] J. Teddy, A. Falqui, A. Corrias, et al., J. Catal. 278 (2011) 59–70.
[19] G.Y. Fan, W.J. Huang, Chin. Chem. Lett. 25 (2014) 359–363.

[20] J. Zhang, F. Lin, L. Yang, Z. He, et al., Chin. Chem. Lett. 31 (2020) 2019–2022.
[21] K. Guo, Y. Liu, M. Han, D. Xu, J. Bao, Chem. Commun. 55 (2019) 11131–11134.
[22] X. Qin, L. Zhang, G.L. Xu, et al., ACS Catal. 9 (2019) 9614–9621.
[23] D. Bernsmeier, M. Bernicke, E. Ortel, et al., J. Catal. 355 (2017) 110–119.
[24] L. Wang, J. Chen, A. Patel, V. Rudolph, Z. Zhu, Appl. Catal. A: Gen. 447–448 (2012) 200–209.
[25] Y. Ma, B. Liu, M. Jing, et al., Chem. Eng. J. 287 (2016) 155–161.
[26] R.S. Suppino, R. Landers, A.J.G. Cobo, Appl. Catal. A: Gen. 525 (2016) 41–49.
[27] D. Gao, S. Li, X. Wang, et al., J. Catal. 370 (2019) 385–403.
[28] P.V. Duc-Ha, C.S. Tan, RSC Adv. 7 (2017) 18178–18188.